TOWARDS REALISTIC SIMULATION OF WAKE-VORTEX EVOLUTION DURING LANDING WITH FLAT AND COMPLEX TERRAIN

Anton Stephan
Institut für Physik der Atmosphäre
Deutsches Zentrum für Luft- und Raumfahrt
(DLR) Oberpfaffenhofen
D-82234 Weßling
Anton.Stephan@dlr.de

Frank Holzäpfel
Institut für Physik der Atmosphäre
Deutsches Zentrum für Luft- und Raumfahrt
(DLR) Oberpfaffenhofen
D-82234 Weßling
Frank.Holzaepfel@dlr.de

Takashi Misaka
Institute of Fluid Science
Tohoku University
2-1-1 Katahira, Aoba-ku
Sendai 980-8577, JAPAN
misaka@edge.ifs.tohoku.ac.jp

ABSTRACT

The complete landing phase of a long range aircraft is studied including final approach, touchdown at the tarmac and the development of the wake. In particular end effects appearing after touchdown and propagating along the wake vortices as well as their interaction with a plate line in front of the run way are investigated. An aircraft model in high lift configuration with deployed flaps and slats obtained from a high fidelity Reynolds-averaged Navier-Stokes simulation is used to simulate the final approach until touchdown. After the wake initialization a large-eddy simulation of the vortical wake is performed until decay. The flow field is analyzed and the interaction with the ground is studied. End effects appear after touch down. They lead to a circulation decay combined with a growth of the core radius to 300%. That effect propagates downstream. The plate line further accelerates the vortex decay reducing rapidly the circulation by another 25% of the initial circulation.

INTRODUCTION

As an unavoidable consequence of lift, aircraft generate a pair of counter-rotating and long-lived wake vortices that pose a risk for following aircraft due to strong coherent flow structures (Gerz *et al.*, 2002). The probability of encountering wake vortices increases significantly during final approach in ground proximity since rebounding vortices may not leave the flight corridor vertically and the possibility of the pilot to counteract the imposed rolling moment is restricted (Holzäpfel & Steen, 2007; Critchley & Foot, 1991). However, less critical encounters are observed than anticipated in wake-vortex advisory systems (WVAS) (Holzäpfel *et al.*, 2011). So the physical mechanisms of wake-vortex evolution and decay after landing still have to be understood.

A landing aircraft generates a highly complex flow field in terms of structure and relevant scales. The flow around an aircraft's main wing, fuselage, slat, flap, jet engine and tail plain, as well as the interaction with the approaching ground and the final crucial lift reduction at the touchdown affect the generated wake vortices. We can divide the evolution of the aircraft's wake during landing into two main phases, (1) wake initialization phase and (2) decay phase of the wake, both separated strictly by the touch down of the aircraft. Whereas phase (1) can be divided into three sub-phases, the roll-up phase, the vortex phase and the decay phase. Usually Reynolds-averaged Navier-Stokes (RANS) simulations are used for the flow around the aircraft and the subsequent roll-up process of the wake in the jet regime (Stumpf, 2005). The dynamics of rolled-up wake vortices until decay have been mainly studied by large-eddy simulations (LES) including various atmospheric conditions of turbulence, stability and wind shear (Holzäpfel *et al.*, 2001; Misaka *et al.*, 2012) Those studies initialize a vortex pair with longitudinally constant velocity profile. This approach for modeling the landing phase was used in Stephan *et al.* (2012). However, it fails to reproduce many characteristic flow features. Measurements for real aircraft landings have also been performed (Holzäpfel & Steen, 2007).

Recent developments in RANS-LES coupling present an innovative methodology to simulate a realistic aircraft flying through a certain domain generating a realistic wake (Misaka *et al.*, 2013). A high-fidelity RANS flow field is sweeped through a LES domain. So a spatial development of the aircraft wake is integrated in a temporal simulation. We use this approach to simulate the aircraft landing and study the physics of the wake-vortex decay.

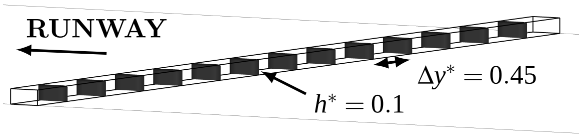

Figure 1. Schematic representation of a plate line of $0.2b_0 \times 0.1b_0$ thin plates with $\Delta y^* = 0.45$ separation.

We study so called end effects appearing after touchdown as a reason for the unexpectedly save aircraft landings.[1] End effects are vortex disturbances that appear in various situations when vortex characteristics change abruptly and weaken the wake vortices when they propagate along the vortices (Bao & Vollmers, 2005; Moet *et al.*, 2005; Stephan *et al.*, 2013). Additionally the interaction of end effects and disturbances caused by plate lines (Stephan *et al.*, 2013) as a method for artificial vortex decay enhancement is investigated. A respective patent entitled “Surface Structure on a Ground Surface for Accelerating Decay of Wake Turbulence in the Short Final of an Approach to a Runway” has been filed under number DE 10 2011 010 147.

METHOD, GOVERNING EQUATIONS

The LES is performed using the incompressible Navier-Stokes code MGLET developed at Technische Universität München for solving the Navier-Stokes equations and the continuity equation (Manhart, 2004)

$$\frac{\partial u_i}{\partial t} + \frac{\partial (u_i u_j)}{\partial x_j} = -\frac{1}{\rho_0}\frac{\partial p'}{\partial x_i} + (\nu_{\mathrm{mol}} + \nu_{\mathrm{turb}})\frac{\partial^2 u_i}{\partial x_j^2} \quad (1)$$

$$\frac{\partial u_j}{\partial x_j} = 0. \quad (2)$$

Here u_i represent the velocity components in three spatial directions ($i = 1, 2$, or 3), and $p' = p - p_0$ equals the deviation from the reference state p_0. The kinematic viscosity is given as the sum of molecular viscosity ν_{mol} and eddy viscosity ν_{turb} defined by means of a Lagrangian dynamic subgrid-scale model (Meneveau *et al.*, 1996). Equations (1) and (2) are solved by a finite-volume approach using a fourth-order finite-volume compact scheme (Hokpunna & Manhart, 2010). A split-interface algorithm is used for the parallelization of the tri-diagonal system (Hokpunna (2009)). A third-order Runge-Kutta method is used for time integration. The simulations are performed in parallel using a domain decomposition approach.

The plate line is modeled by introducing a drag force source term $F_{D,i} = C_D|u|u_i$ with a large drag coefficient in the region of the plate, Fig. 1. At the ground surface of the LES domain we employ the Grötzbach wall model that locally computes the wall shear stress τ_w based on the logarithmic law (Grötzbach, 1987).

[1] http://www.youtube.com/watch?v=PpUftG_mxg8

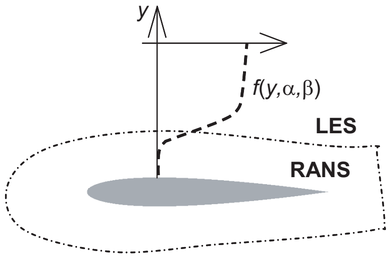

Figure 2. Schematic of a weighting function for a combination of RANS and LES flow fields.

WAKE INITIALIZATION

We employ a wake initialization approach where a realistic aircraft wake is generated in a LES domain by sweeping a high-fidelity RANS flow field through the domain, which enables to simulate the wake-vortex evolution from generation until final decay (Misaka *et al.*, 2013). The simulations are performed for a large transport aircraft model in high-lift configuration used in ONERA’s catapult facility during the European AWIATOR project. The RANS flow field serves as a forcing term of the Navier-Stokes equations in the LES. This approach might be referred to as a fortified solution algorithm (Fujii, 1995), or a nudging technique used in data assimilation (Kalnay, 2003). The resulting velocity field in the aircraft vicinity consists of the weighted sum

$$\mathbf{V} = f(y)\mathbf{V}_{\mathrm{LES}} + (1 - f(y))\mathbf{V}_{\mathrm{RANS}} \quad (3)$$

of the LES and the RANS velocity field, see Fig 2, with a transition function

$$f(y, \alpha, \beta) = \frac{1}{2}\left[\tanh\left[\alpha\left(\frac{y}{\beta} - \frac{\beta}{y}\right)\right] + 1.0\right]. \quad (4)$$

Here α and β represent slope and wall-distance of the transition, chosen similar to the values in Misaka *et al.* (2013). In addition the wall-distance parameter $\beta = 0.08$ is gradually reduced depending on the wall distance beneath the aircraft to $\beta = 0.013$. This way we take account for the wing-in-ground effect which is not considered in the RANS solution.

The mapping of the RANS flow field from an unstructured, mesh refined grid to the structured LES domain is performed by a linear interpolation once before the wake initialization. Thirty-two RANS fields are used alternately to achieve a realistically small descent angle. Hence, additional memory is required. However, few additional computation cost is required.

APPROACH AND BOUNDARY TREATMENT

The present approach is shown schematically in Fig. 3. In the simulations, the aircraft approaches the ground with an angle of 3.57 degree. The angle of attack of the fuselage equals 5.54 degree.

At the instant of touchdown the lift ceases quickly, when suddenly the bound vortex, i.e. the circulation around the aircraft wings, as well as the wake vortices vanish. After touchdown the aircraft

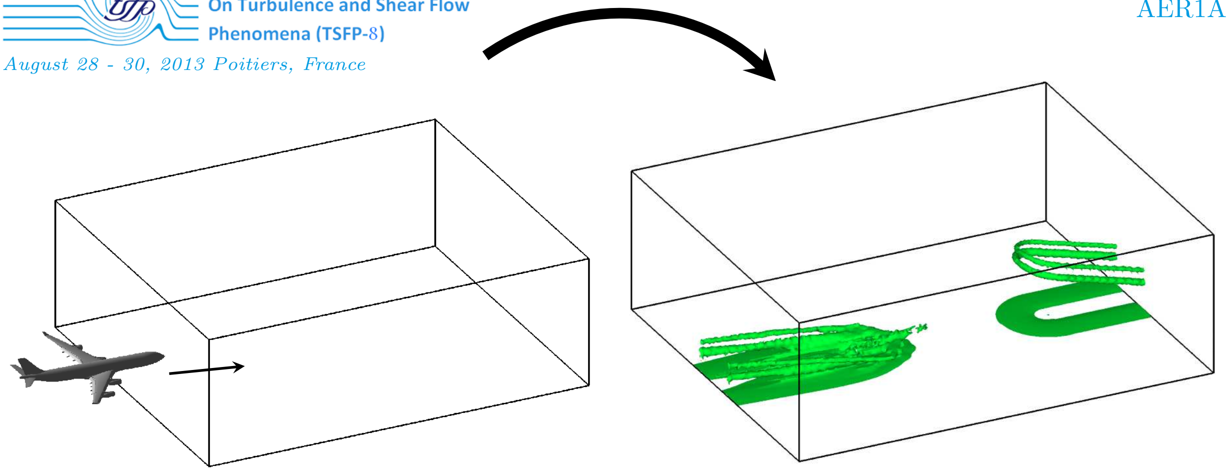

(a) Wake initialization until touchdown.

(b) LES, vortex decay after touchdown.

Figure 3. Schematic of aircraft landing, (a) wake initialization, (b) artificial vortex reconnection and wake evolution after touchdown.

wake can be regarded as white noise (Hah & Lakshminarayana, 1982). We model the touchdown just by removing the RANS flow field forcing term from the simulation and do not take into account the white noise wake of the rolling aircraft. We employ periodic boundary conditions in horizontal directions. A no-slip condition at the ground and a free-slip condition at the top side. The aircraft starts in the back part of the domain passes the boundary and approaches the ground. After touchdown the first slice of the domain is prolongated into the back part continuing the slope of the vortex and closed artificially to a half ring, Fig. 3 (b). This procedure is important to avoid disturbances generated at the starting point of vortex initialization.

COMPUTATIONAL SETTING

We employ a RANS flow field obtained by the DLR TAU-code with an adaptive mesh refinement for wingtip and flap vortices as well as the fuselage wake. The flow conditions of the RANS simulation are the same as in ONERA's catapult facility experiment, i.e. Reynolds number $\mathrm{Re} = 5.2 \times 10^5$, free stream velocity respectively flight speed $U_\infty = 25\,\mathrm{m/s}$, and a lift coefficient $C_L = 1.4$. The 1/27 scaled model has a wingspan of $2.236\,\mathrm{m}$. We normalize quantities with the following reference values, initial circulation, vortex spacing, vortex descent velocity, and characteristic time, for an elliptic load distribution (Gerz *et al.*, 2002),

$$\Gamma_0 = \frac{2C_L U_\infty b}{\pi\Lambda}, \quad b_0 = \frac{\pi}{4}b, \quad w_0 = \frac{\Gamma}{2\pi b_0}, \quad t_0 = \frac{b_0}{w_0} \tag{5}$$

with a wing aspect ratio of $\Lambda = 9.3$. The resulting reference values for the normalization are $\Gamma_0 = 5.36\,\mathrm{m^2/s}$ for circulation, $b_0 = 1.756$ for length, $w_0 = 0.49\,\mathrm{m/s}$ for velocity, and $t_0 = 3.617\,\mathrm{s}$ for time. We set $t = 0$ at the instant of the touchdown.

In the LES we employ uniform mesh spacing for all three spatial directions, with a resolution of $\Delta^* = dx^* = dy^* = dz^* = 0.011$, comparable to mesh spacing in Misaka *et al.* (2013). Hence, the out of ground effect behavior of the wake vortices should be similar to Misaka *et al.* (2013). The dimensions of the complete computational domain are $23.3b_0$, $5.8b_0$, and $2.2b_0$ in flight, span and vertical directions, respectively. The backpart with a length of $5b_0$ is used for aircraft starting and the half ring closing. At touchdown the tail wing is at $x^* = 16.3$, the plate line is centered at $x^* = 5.1$.

FLOW FIELD, END EFFECTS

According to Misaka *et al.* (2013) the wake behind the aircraft wings consists of a complex vorticity distribution in the near-field, see Fig. 4. However, only a few vortices remain behind the tail wings, wing- and flap-tip vortices, as well as vortices from the wing-fuselage junction, clearly visible in Figs. 4 (a)-(d). Wing- and flap-tip vortices merge at a distance of about $x^* = 13$ from the aircraft, Fig. 4 (c). The wake vortices as well as the bound vortex induce a vorticity layer of opposite sign at the ground surface, first the wake vortices and later the bound vortex at the aircraft wings, Figs. 4 (a),(b). The effect of the plate line disturbing the secondary vorticity layer is visible in Fig. 4 (c). Shortly after touchdown the bound vortex vanishes and the ends of the wake vortices start to interact with the vorticity layer at the ground, disturbing the wake vortices starting from the point of touchdown. This process constitutes the end effects propagating as helical disturbances along the wake vortices, see Figs. 4 (d)-(h). Port- and starboard-vortices are no longer linked by the bound vortex and quickly diverge at the point of touchdown, Figs. 4 (e)-(h).

Additionally we observe a linking of the vortex ends with the ground. The secondary vorticity layer induced by the descending wake vortices rolls up to secondary vortex structures as detailed in Stephan *et al.* (2013). This process starts above the plate line, Figs. 4 (f),(g). The secondary vortex structures wind around the primary vortices and propagate by self-induction in axial directions to both sides. These helical disturbances finally interact with the end effects.

The turbulent structures generated by the fuselage, Figs. 4 (a)-(c), are stretched around the primary vortices and are quickly transported to the ground between the vortex pair disturbing the relatively smooth shape of the secondary vorticity layer, Figs. 4 (e)-(h).

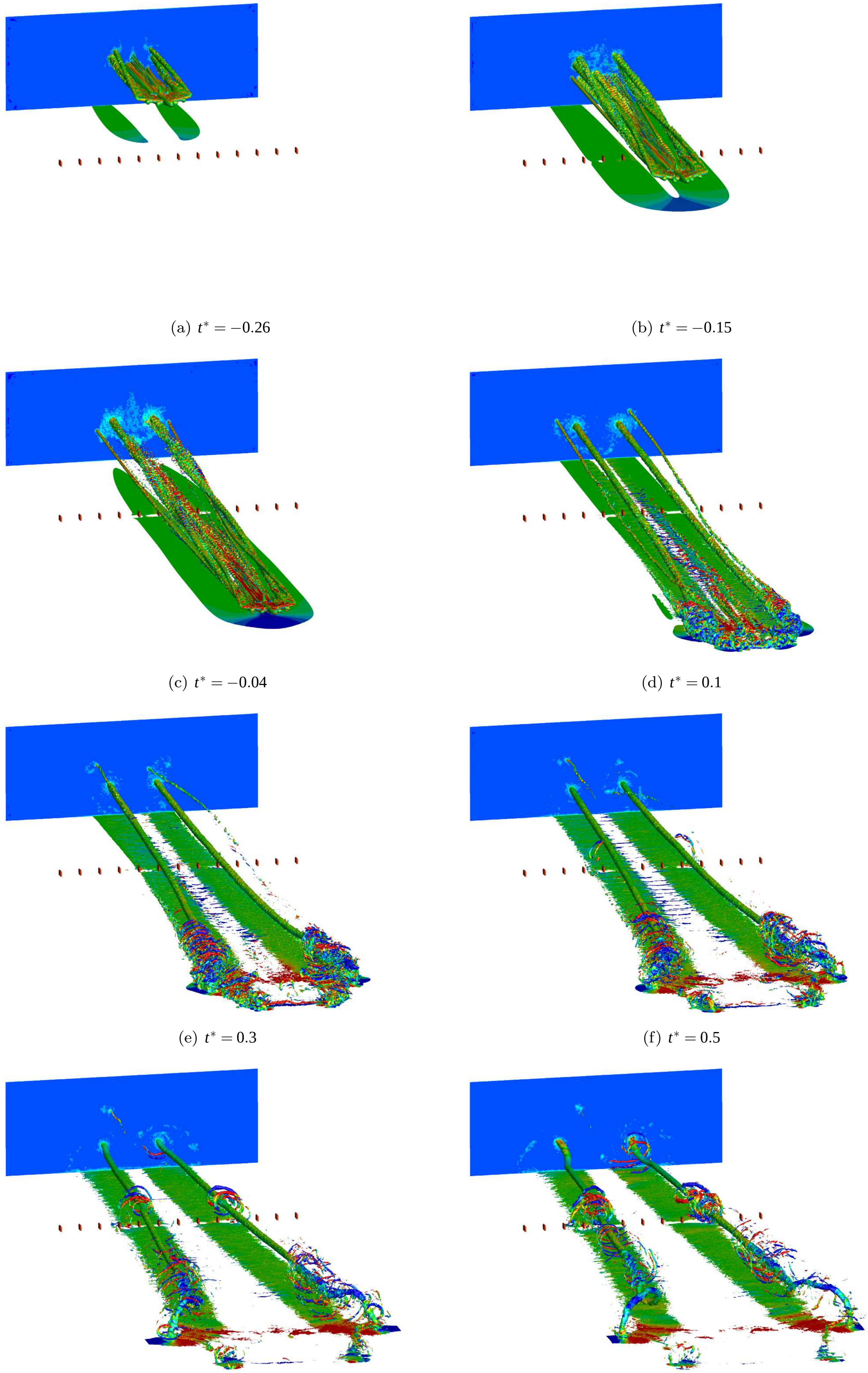

(a) $t^* = -0.26$ (b) $t^* = -0.15$

(c) $t^* = -0.04$ (d) $t^* = 0.1$

(e) $t^* = 0.3$ (f) $t^* = 0.5$

(g) $t^* = 0.73$ (h) $t^* = 0.98$

Figure 4. Aircraft landing with roll-up, approach, touchdown, plate line, and developing end effects. Iso-vorticity surface $||\omega^*|| = 110$ colored with vorticity in spanwise direction.

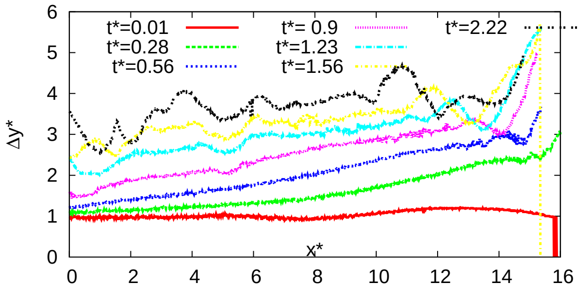

Figure 5. Vortex spacing at different vortex ages, plate line effect.

Hence, the secondary vortices are disturbed in their development generating irregularities. The counter-rotating secondary vortices finally develop into relatively strong turbulent structures initiating rapid vortex decay of the primary vortices, see Stephan *et al.* (2013).

VORTEX DIVERGENCE

Wake vortices diverge in ground proximity. During the landing, the divergence is not uniform, but starts at the point of touchdown and proceeds downstream, as depicted in Fig. 5. The plate line slightly decelerates the divergence. Maximum vortex separation of $5.8b_0$ is reached at the domain boundary, hence we may expect even larger vortex separations close to the touchdown area in a larger simulation domain.

VORTEX DECAY AND CORE RADIUS

Of particular interest is the vortex strength that ultimately might affect a following aircraft. As a common measure of the vortex intensity for aircraft with sufficiently large wingspans, we consider $\Gamma_{5-15} = 0.1\int_{5\,\mathrm{m}}^{15\,\mathrm{m}} \Gamma(r)dr$ for the primary vortices, where $\Gamma(r) = \oint \vec{u}\cdot d\vec{s}$ denotes the circulation around a circle of radius r centered in the vortex core (Holzäpfel *et al.*, 2001). After vortex initialization at the instant of touchdown we have a nearly constant circulation slightly lower than Γ_0 over the entire domain increasing slightly in the region of the RANS field at touch down, see Fig. 6 (a). We clearly see the end effects after touch down, leading to a circulation decay starting from the very ends of the wake vortices. The disturbance propagates until the end of the domain. In the case without the plate line the decay proceeds uniformly. The effect of the plate line is clearly visible in Fig. 6 (b). Above the plate line the circulation decay is initiated propagating subsequently to either side. The disturbances from the end effects as well as from the plate line superpose, leading to a more vigorous decay. In the region of the plate line we have a reduction of the circulation to less than 50%, whereas in case without the plate line the circulation falls to 70 % at $t^* = 2.2$, see Fig. 7.

The core radius, which is initially a bit too high, due to resolution limitations, increases drastically after touchdown. Together with the circulation decay the end effect causes an augmentation of the core radius to 300% of the initial value. Note that the interaction of the end effect and the disturbance coming from the plate line leads to intriguing behavior of the core radius. The growth of the core radius is suppressed in the region of the plate line, however it continues in a certain distance. The end effects propagate with an approximately constant speed of $U^*_{\mathrm{prop}} = 7.1$ up to a time of $t^* = 2$.

CONCLUSION, DISCUSSION, OUTLOOK

A complete landing phase of an long range aircraft including approach, touchdown, and the evolution of the wake was simulated combining RANS and LES flow fields. The RANS flow field was used as a forcing term in the ground fixed LES domain. The aircraft was in high lift configuration with flaps and slats deployed. In addition the effect of a plate line posed in front of the runway was investigated. The complex flow field of a landing aircraft particularly the different vortices constituting the wake were visualized and analyzed. The vortex separation in ground proximity was quantified. End effects occurring after touch down were studied. They lead to a circulation decay combined with a core radius growth. Rapid circulation reduction caused by the plate line demonstrates the benefits of plate lines in front of the runway.

Since the landing process was approximated by one stationary RANS field, the instant of touch down is not simulated very accurately. As a consequence end-effects are initiated later than it is expected in reality. It is planed to employ a series of URANS fields for the touch down in future. The investigated angle of approach of 3.56 degree is to high compared to 3 degree as a standard in aviation. As a consequence the effect of the plate line should be even more pronounced at an airport. The effect of a turbulent wind during the landing will also be investigated in future.

ACKNOWLEDGMENTS

We would like to thank Stefan Melber (Institut für Aerodynamik und Strömungstechnik, DLR-Braunschweig) for providing the RANS data of the AWIATOR long range aircraft model. We also thank Airbus for the allowance to use it. We thank Prof. Michael Manhart and Dr. Florian Schwertfirm for the provision of the original version of the LES code MGLET. Computer time provided by Leibniz-Rechenzentrum (LRZ) is greatly acknowledged.

REFERENCES

Bao, F. & Vollmers, H. 2005 Alleviation of end-effects in facilities for far wake investigations. In *AIAA-Paper 205-0907, 43rd AIAA Aerospace Sciences Meeting and Exhibit*. Reno, Nevada, USA.

Critchley, J. & Foot, P. 1991 UK CAA wake vortex database: Analysis of incidents reported between 1982 and 1990. *Civil Aviation Authority, CAA Paper* **91**.

Fujii, K. 1995 Unified zonal method based on the fortified solution algorithm. *Journal of Computational Physics* **118**, 92–108.

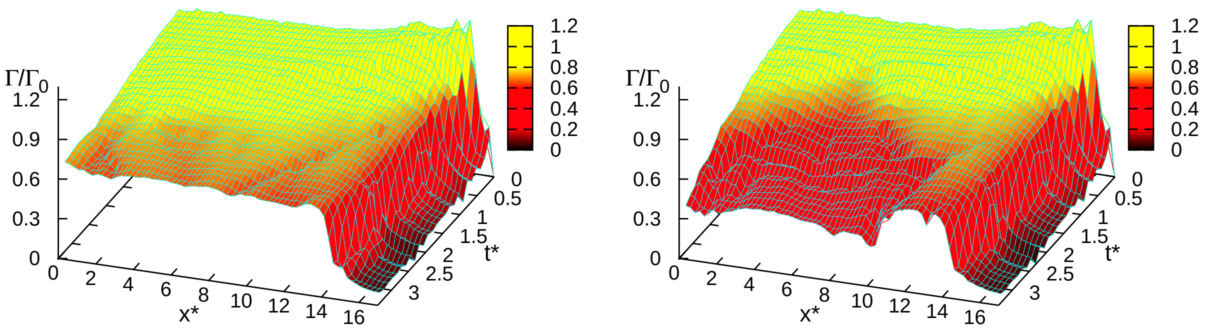

Figure 6. Vortex circulation (Γ_{515}) distribution evolution after touchdown, effect of a plate line (right).

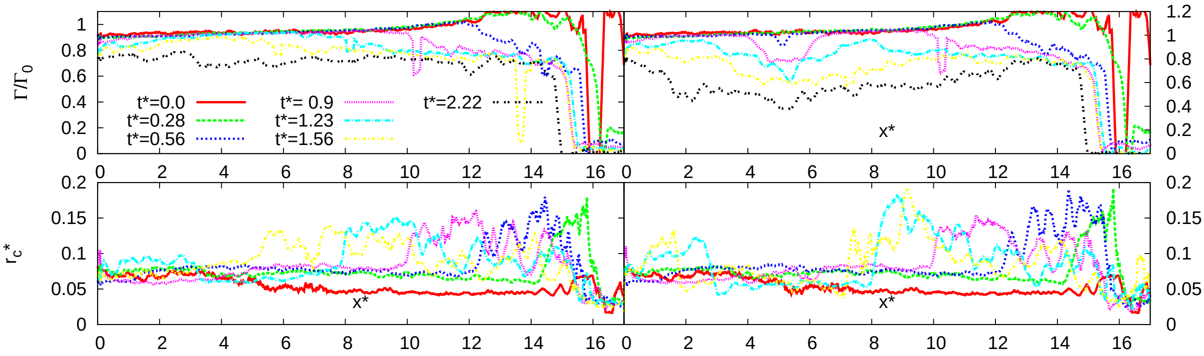

Figure 7. Vortex circulation (Γ_{515}) distribution and core radius evolution no plate line (left), plate line (right).

Gerz, T., Holzäpfel, F. & Darracq, D. 2002 Commercial aircraft wake vortices. *Progress in Aerospace Sciences* **38** (3), 181–208.

Grötzbach, G. 1987 Direct numerical and large eddy suimulations of turbulent channel flows. In *Encyclopedia of fluid mechanics (ed. N. Cheremisinoff)*, pp. 1337–1391. Gulf Publishing Company, Houston, Texas.

Hah, C. & Lakshminarayana, B 1982 Measurement and prediction of mean velocity and turbulence structure in the near wake of an airfoil. *Journal of Fluid Mechanics* **115**, 251–282.

Hokpunna, A. 2009 Compact fourth-order scheme for numarical simulations of navier-stokes equations. PhD thesis, Technische Universität München (Germany).

Hokpunna, A. & Manhart, M. 2010 Compact fourth-order finite volume method for numarical solutions of navier-stokes equations on staggered grids. *Journal of Computational Physics* **229** (20), 7545–7570.

Holzäpfel, F., Dengler, K., Gerz, T. & Schwarz, C. 2011 Prediction of dynamic pairwise wake vortex separations for approach and landing. In *AIAA-Paper 2011-3037, 3rd AIAA Atmospheric Space Environments Conference*. Honululu, Hawaii, USA.

Holzäpfel, F., Gerz, T. & Baumann, R. 2001 The turbulent decay of trailing vortex pairs in stably stratified environments. *Aerospace Science and Technology* **5** (2), 95–108.

Holzäpfel, F. & Steen, M. 2007 Aircraft wake-vortex evolution in ground proximity: Analysis and parameterization. *AIAA Journal* **45**, 218–227.

Kalnay, E. 2003 *Atmospheric Modeling, Data Assimilation and Predictability*. Cambridge University Press.

Manhart, M. 2004 A zonal grid algorithm for dns of turbulent boundary layer. *Computer and Fluids* **33** (3), 435–461.

Meneveau, C., Lund, T. S. & Cabot, W. H. 1996 A lagrangian dynamic subgrid-scale model of turbulence. *Journal of Fluid Mechanics* **319**, 353–385.

Misaka, T., Holzäpfel, F. & Gerz, T. 2013 Wake evolution of high-lift configuration from roll-up to vortex decay. In *AIAA-Paper 2013-0362, 51st AIAA Aerospace Sciences Meeting*. Grapevine, Texas, USA.

Misaka, T., Holzäpfel, F., Hennemann, I. Gerz, T., Manhart, M. & Schwertfirm, F. 2012 Vortex bursting and tracer transport of a counter-rotating vortex pair. *Physics of Fluids* **24**, (025104–1) – (025104–21).

Moet, H., Laporte, F., Chevalier, G. & Poinsot, T. 2005 Wave propagation in vortices and vortex bursting. *Physics of Fluids* **17**, 054109.

Stephan, A., Holzäpfel, F. & Misaka, T. 2012 Aircraft wake vortex decay in ground proximity - physical mechanisms and artificial enhancement. In *AIAA-Paper 2012-2672, 4th AIAA Atmospheric and Space Environments Conference*. New Orleans, Luisianna, USA.

Stephan, A., Holzäpfel, F. & Misaka, T. 2013 Aircraft wake vortex decay in ground proximity - physical mechanisms and artificial enhancement. *Journal of Aircraft* **accepted**.

Stumpf, E. 2005 Study of four-vortex aircraft wakes and layout of corresponding aircraft configurations. *Journal of Aircraft* **42**, 722–730.